

CRSUS, Volume 1

Supplemental information

**Planning charging stations for 2050 to support
flexible electric vehicle demand considering
individual mobility patterns**

Jiaman Wu, Siobhan Powell, Yanyan Xu, Ram Rajagopal, and Marta C. Gonzalez

Supplemental Experimental Procedures

Note S1: Sensitivity Analysis

We test the performance of our personalized recommendations with three parameters, i.e., maximum shifting stays, different peak hours, and recommendation acceptance rates.

- **Maximum Shifting Stays:** Maximum shifting stay is the maximum number of stays we assume each session can be shifted from the original charging session. We set different maximum shifting limits to test how shifting by fewer stays would influence the success of the peak shaving results. We find in Fig. 1 (a) that, consistently under different EV adoption rates, larger maximum shifting stays enable more peak shaving, and even with a maximum displacement of 2 stops (stays) the recommendations are able to achieve more than 40% shaving.
- **Different Peak Hours:** Different peak hours are the possible period of grid peak hours. In the future, the increasing production from renewables and the availability of other system management assets will cause the peak of the net load on the grid to occur at different times of day. In this sensitivity analysis, we test how different peak hours will influence the success of the algorithm's peak shaving results. We test four cases: morning, afternoon, evening, and late-time peak periods. We find in Fig. 1 (b) that the morning peak hour benefits from the most shaving and the midnight peak hour benefits from the least shaving. This happens because the current uncontrolled charging peak occurs in the morning or afternoon/evening, so the morning/afternoon/evening peak has more potential to be shaved. Also, since current home charging access is higher than work charging access, moving workplace charging (which usually happens in the morning) to home charging (which usually happens in the afternoon/evening) is easier than moving home charging to workplace charging.
- **Recommendation Acceptance Rate:** Recommendation acceptance rate is the ratio of drivers who follow the recommendations. In the base case we assume all drivers follow the personalized shifting recommendations in this work. In practice, adopters may not follow the personalized shifting recommendations for personal reasons. We vary the ratio of drivers who follow the recommendations to test how different levels of compliance will influence the peak shaving results. We confirm in Fig. 1 (c) that with an increasing fraction of drivers following the recommendations, peak shaving is more successful. When the acceptance rate is just 20%, the recommendations can still achieve over 10% shaving. Designing incentives and education programs to increase recommendations following ratio is necessary to realize the full potential of this demand flexibility.

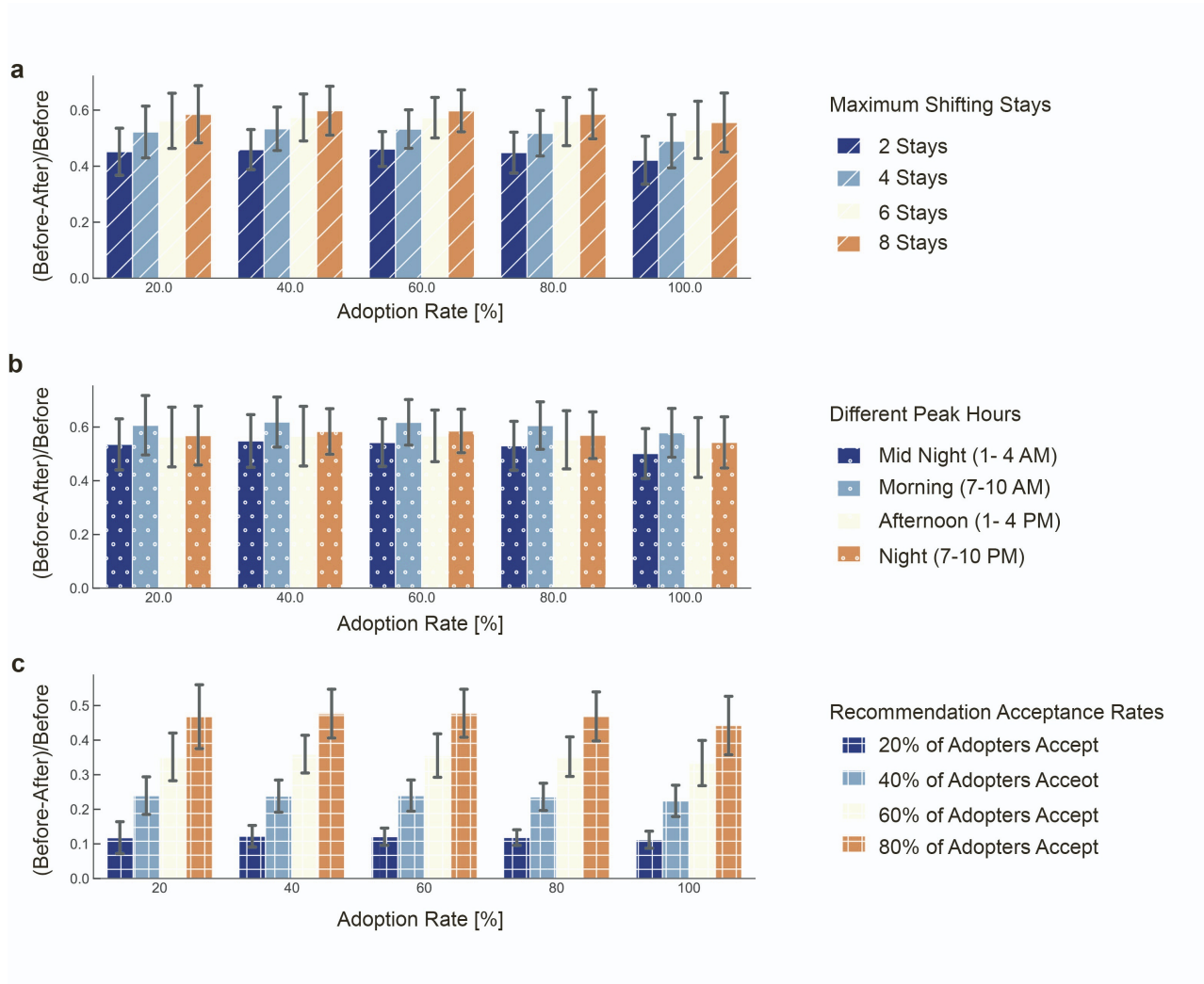


Figure 1: Sensitivity analysis of personalized shifting recommendations. We show ZIP code level differences between before and after our personalized shifting recommendations in the ratio of before recommendations under different EV adoption rates. The error bar highlights the variance among ZIP codes. (a) Peak shaving effects under different maximum numbers of shifting stays. (b) Peak shaving effects under different peak hours. (c) Peak shaving effects under different recommendation acceptance rates.

Note S2: Unbalanced Demand with Increasing Adoption Rates

With increasing adoption rates, ZIP codes in Bay Area show sub-linear increases and super-linear increases in peak charging loads. We identify sub-linear and super-linear increases in peak charging load on the ZIP code level and visualize the increases in Figure 2 and Figure 3. Sub-linear growth in a given ZIP code indicates there is less EV demand there from early adopters and more from later adopters; super-linear growth means the opposite.

Figure 2 shows the average peak charging loads with increasing adoption rates for ZIP codes with sub-linear and super-linear increases in load respectively. The dashed line shows the linear increase of the peak charging load. The solid line above the dashed line represents the average load of ZIP codes with sublinear increases while the solid line below the dashed line represents the average load of ZIP codes with superlinear increases. Figure 2 a and c show that during grid peak hours, the shifting strategy narrows the gap of load between sub-linear increasing ZIP codes and super-linear increasing ZIP codes. In contrast, Figure 2b and d show that during grid off-peak hours, the shifting strategy enlarges the gap of load between sub-linear increasing ZIP codes and super-linear increasing ZIP codes.

Figure 3a-b indicate more sublinear increases in South Bay Area and more superlinear increases in North Bay Area. The difference among ZIP codes implies the unbalanced development of EV charging demand in the Bay Area. Figure 3c indicates that the recommendations reduce the number of ZIP codes with sublinear increases in South Bay Area during grid peak hours. Figure 3d shows that the recommendations reduce the number of ZIP codes with superlinear increases in North Bay Area and increase the number of ZIP codes with sublinear increases in South Bay Area during grid off-peak hours.

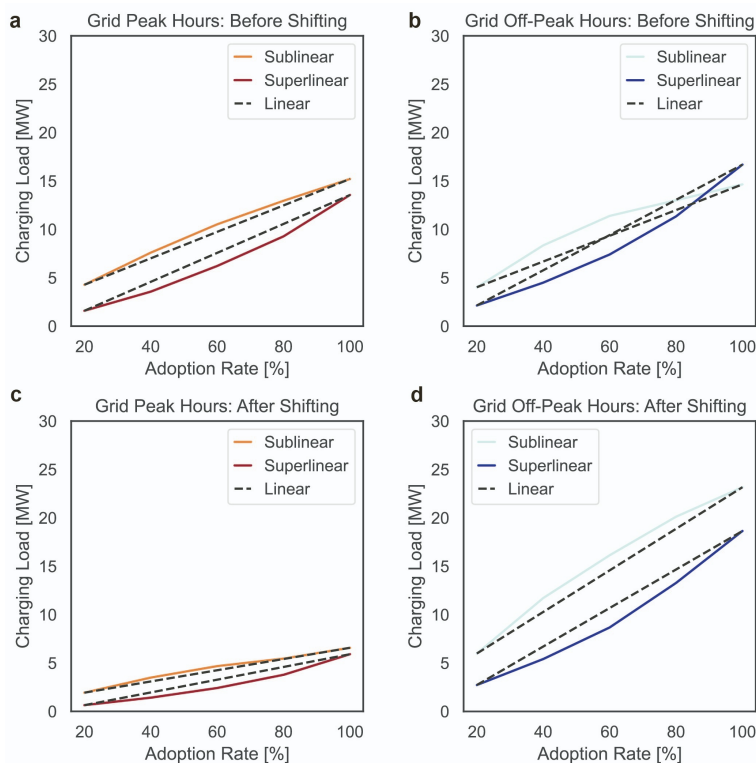


Figure 2: Sub-linear increase and super-linear increase in peak charging needs.

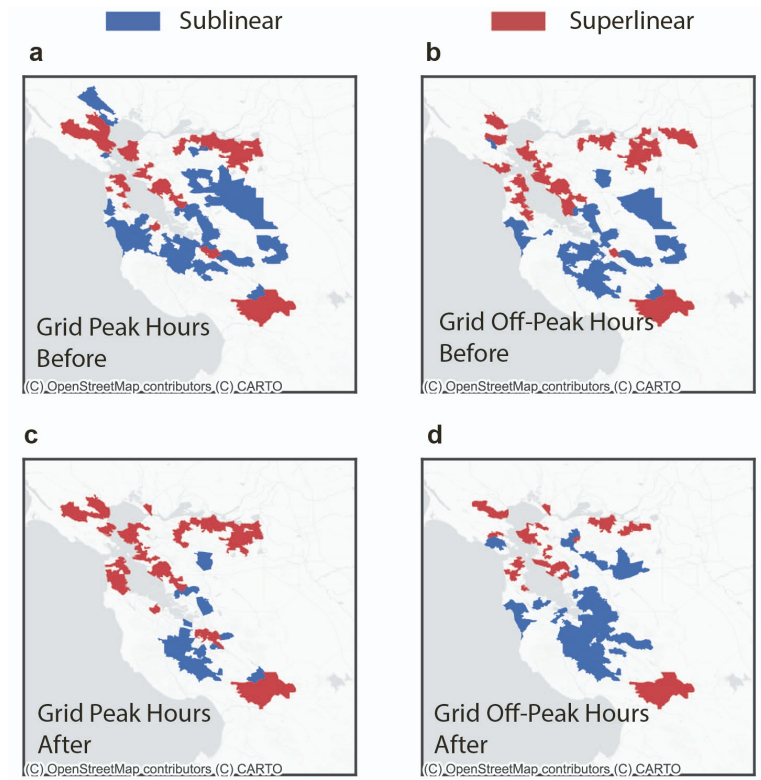


Figure 3: Sub-linear increase and super-linear increase in peak charging needs.

Note S3: EV models market share

Figure 4 shows the market share of battery-operated EVs used in this study [1]. We observe that Tesla Model 3 and Nissan LEAF S are the most popular model. The Tesla Model 3 has a battery capacity of 50-82 kWh and Nissan LEAF S has a battery capacity of 40 kWh [3].

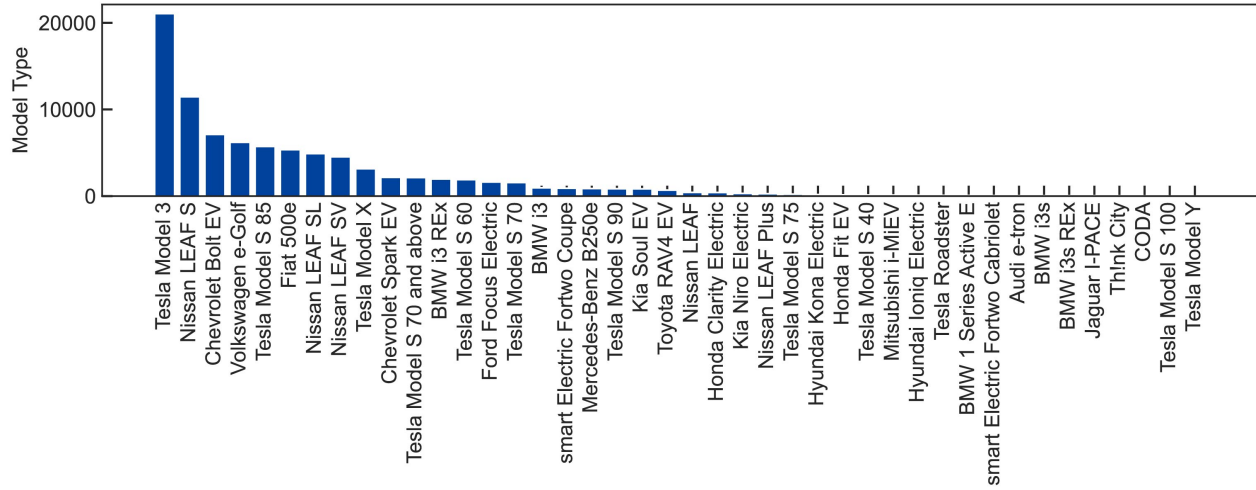


Figure 4: BEV models market share.

Note S4: Travel behavior of the EV drivers

Figure 5a shows the distribution arrival time for EV drivers in the year 2019. There are two peaks during the day. One happens at around 9 a.m. in the morning, while the other happens at around 7 p.m. at night. Figure 5b shows the departure time distribution. The distribution of arrival time and departure time are similar since people spend little time on the way. The histogram of daily energy consumption is shown in Fig. 5c. Most people consume less than 25 kWh a day. Figure 5d shows the number of stays during the day. Most people visit two places during the day.

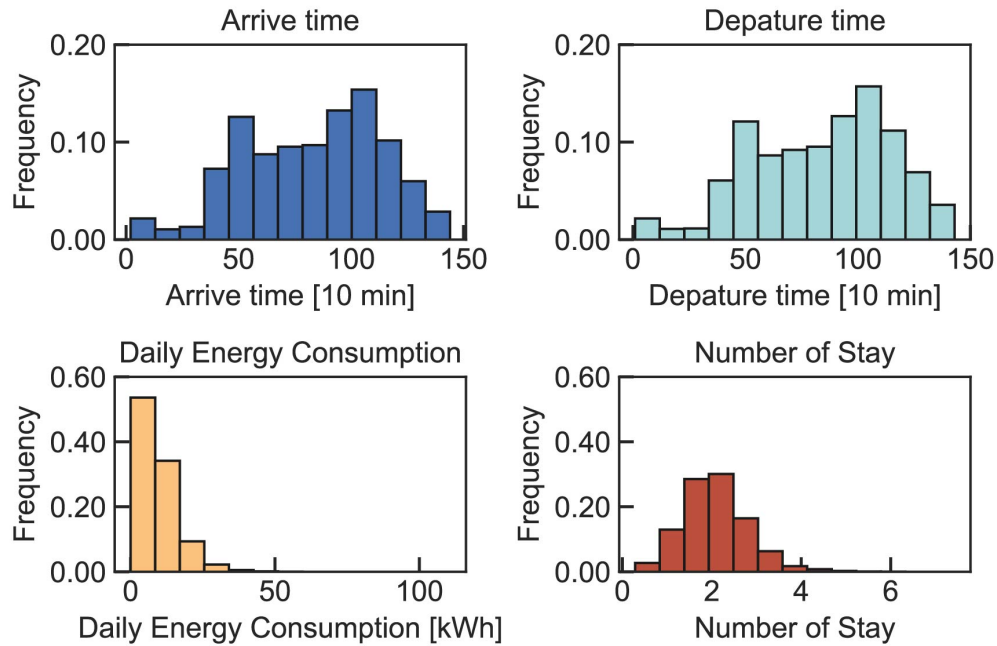


Figure 5: Statistics illustrating the simulated travel behavior of all users.

Note S5: Speech Groups Data

The dendrograms in Fig. 6 and Fig. 7 illustrate the result of the hierarchical clustering on real charging data with 136 charging groups. Some statistics are annotated to support the labeling interpreting the clustering results.

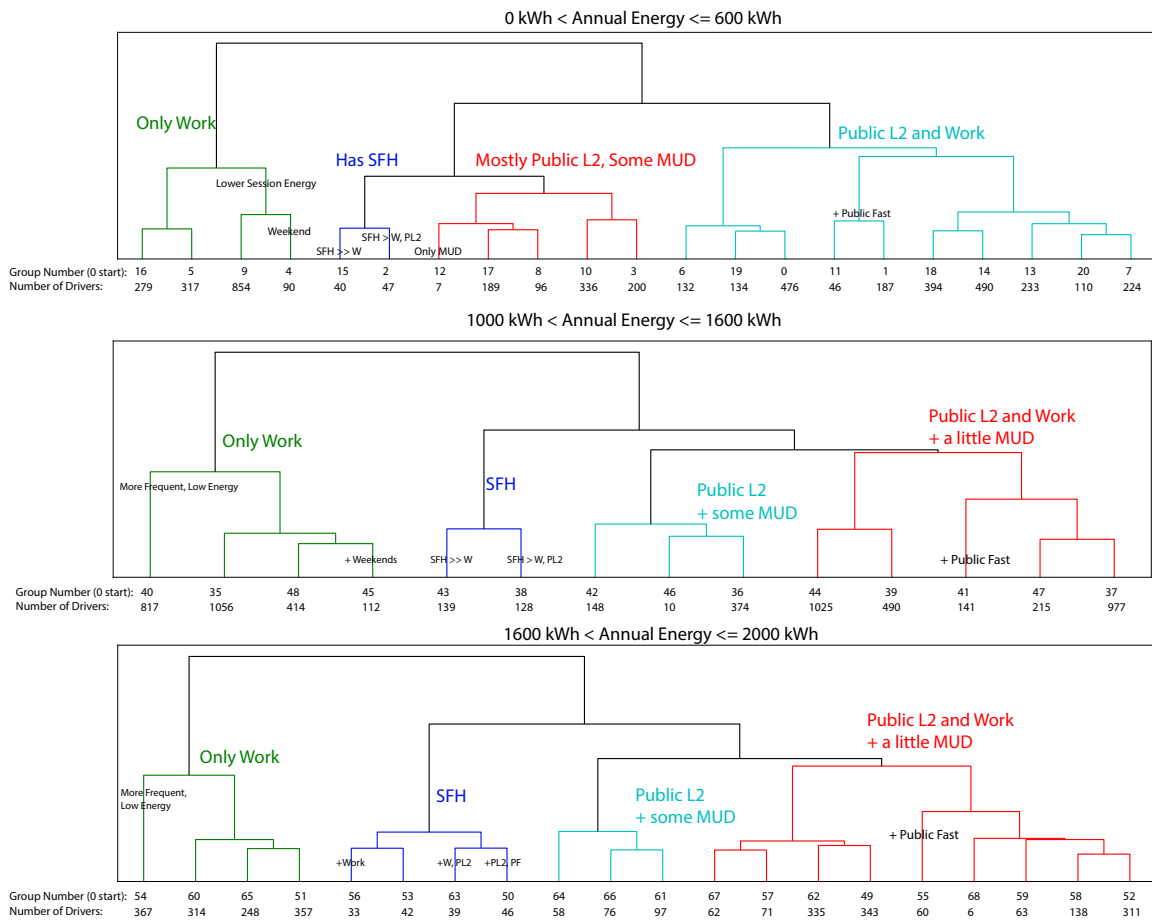


Figure 6: Speech Groups Clustering Dendrograms (Group from 1 to 68)

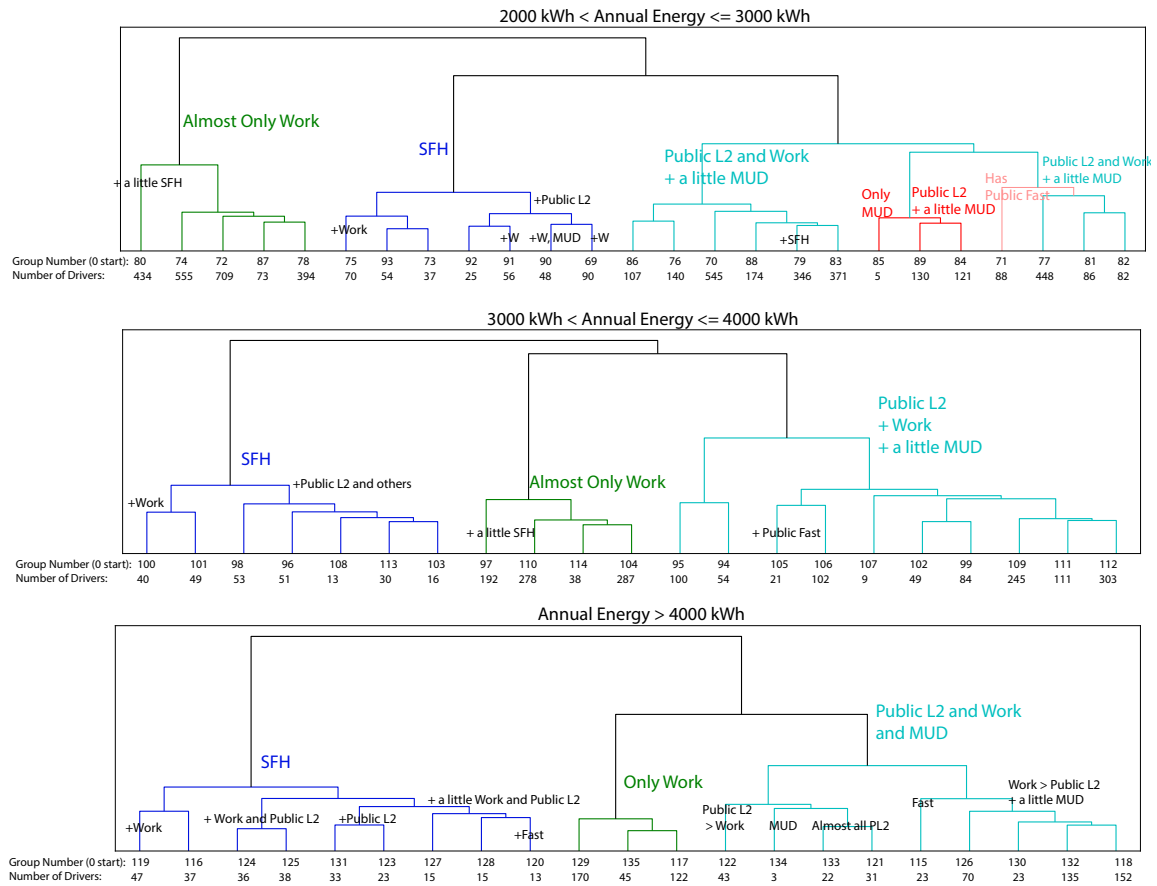


Figure 7: Speech Groups Clustering Dendrograms (Group from 69 to 136)

Note S6: Home charging access survey Data

Table 1 shows the share of vehicles that currently park near 120V electricity or could park in locations where respondents think new electrical installation could occur [2]. We observe that people living in SFH with higher household incomes have a higher probability to have home charging access.

Household Income	\$ 60,000 or less	\$ 60,000 or less	\$ 60,000 to \$100,000	\$ 60,000 to \$100,000	\$ 100,000 or More	\$ 100,000 or More
Housing Type	SFH	MFH	SFH	MFH	SFH	MFH
Potential Access with Parking Behavior Modification	72%	29%	78%	36%	85%	43%

Table 1: Data from the California Energy Commission's Home Charging Access Survey [2].

Note S7: Monte Carlo simulation

For each EV adopter, TimeGeo estimates when and where the adopter visit during the week. We apply the Algorithm 1 to estimate the charging behavior of a given EV adopter.

Algorithm 1 Monte Carlo simulation for one EV adopter

Input: G : charging group of the adopter, where $G \in [1, \dots, 136]$;

e : weekly energy consumption of the adopter;

t : stay period of the adopter, where $t_i = (t_i^a, t_i^d)$ with t_i^a and t_i^d as arrival time and departure time, respectively, $t_i^a, t_i^d \in [1, \dots, 1008]$;

l : stay place of the adopter, where $l_i = (l_i^{type}, l_i^{coordinates})$ with $l_i^{type} \in [\text{home}, \text{work}, \text{public}]$;

$P(z | G)$: the probability of an adopter charging in the charging segment z given the charging behaviour group G in a day, where $z \in [\text{SFH L1}, \text{SFH L2}, \text{MFH L2}, \text{Work L2}, \text{Public L2}, \text{Public L3}]$;

$P(c | G, z)$: the Gaussian mixture model of charging energy of an adopter in a given group G charging in each segment z on a day, where $c \in \mathbb{R}^+$.

Output: t^* ; l^* : when and where the adopter charges;

c^* : energy charged in the stay;

z^* : charging segment in the stay.

```
1: for stay  $i$  in all stays do
2:
3:   // When and where charging happens
4:    $t_i^* = t_i$ ;  $l_i^* = l_i$ 
5:
6:   // How to charge (charging segment in the session)
7:   if  $l_i^* \in [\text{home}]$  then
8:      $z_i' = [\text{SFH L1}, \text{SFH L2}, \text{MFH L2}, \text{Public L2}, \text{Public L3}]$ 
9:   else if  $l_i^* \in [\text{work}]$  then
10:     $z_i' = [\text{Work L2}, \text{Public L2}, \text{Public L3}]$ 
11:  else if  $l_i^* \in [\text{public}]$  then
12:     $z_i' = [\text{Public L2}, \text{Public L3}]$ 
13:  end if
14:   $z_i^* = \max_{z_i' \in z_i'} P(z_i' | G)$ .
15:  Sample if the driver charges in segment  $z_i^*$  with probability  $P(z_i^* | G)$ .
16:
17:  // How much to charge (charging energy in the session)
18:  if the driver charges in segment  $z_i^*$  then
19:    Sample the energy charged with Gaussian mixture model  $c_i^* = P(c_i | G, z_i^*)$ .
20:  else
21:     $c_i^* = 0$ 
22:  end if
23: end for
24:  $c_i^* = (c_i^* / \sum_j c_j^*) \times e$ 
25: return  $t^*, l^*, c^*, z^*$ 
```

Note S8: Validation for adoption model in the year 2019

Figure 8 shows a comparison between the CVRP data [1] and our simulation. Figure 8a and 8b show the geographical distribution of CVRP and our simulation. The distributions are similar in most ZIP codes. Figure 8c shows the correlation between CVRP data and our simulation, which implies a good agreement between the number of EVs obtained via the Bayesian estimates and the mobility model versus the ground truth of EV usage.

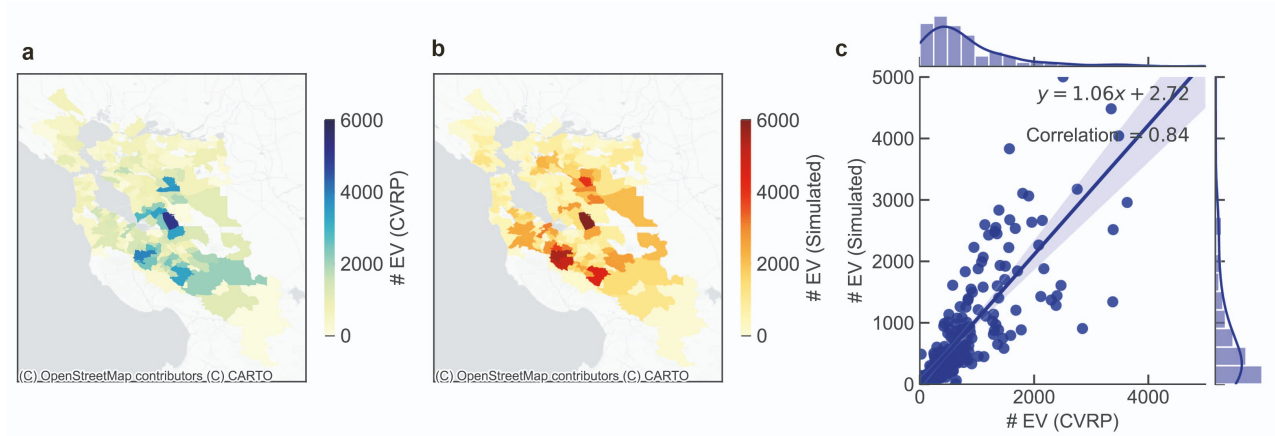


Figure 8: Validation for adoption model in the year 2019.

Note S9: Geographical distribution of EV adopters with increasing adoption rate

Figure 9 shows the number of EV drivers with an increasing adoption rate. The early EV adopters locate in the South Bay as shown in Fig. 9a-c. When the adoption rate keeps increasing, there will be more EV adopters in the North Bay Area as shown in Fig. 9d-f.

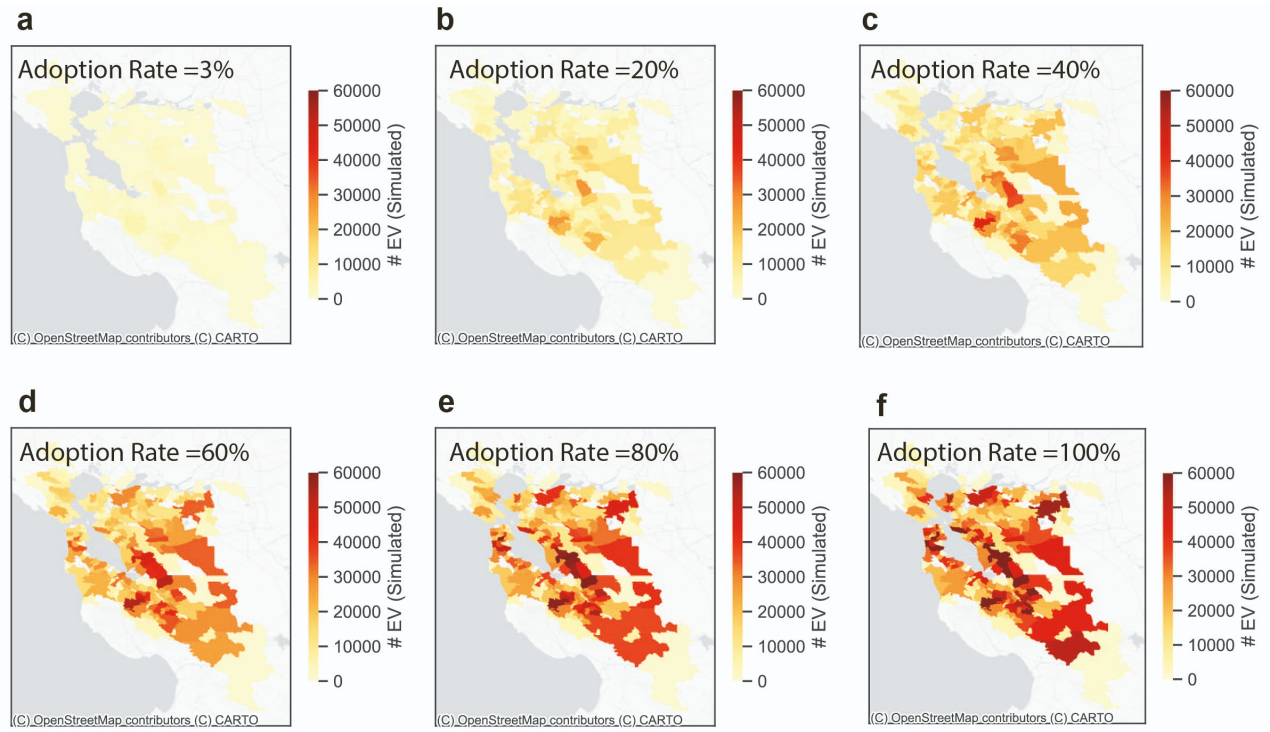


Figure 9: Geographical distribution of EV adopters with increasing adoption rate

References

- [1] California Center for Sustainable Energy. California air resources board clean vehicle rebate project. <https://cleanvehiclerebate.org/en/rebate-statistics>, Feb 2022. Accessed on Feb. 2, 2022.
- [2] California Energy Commission. Home charging access in california. <https://www.energy.ca.gov/publications/2022/home-charging-access-california>, 2022. Accessed on May 1, 2022.
- [3] Electric Vehicle Database. 2023 current and upcoming electric vehicles. <https://ev-database.org/>. Accessed on March 1, 2023.